Seismic Retrofitting of RC Buildings Using CFRP and Post-Tensioned Metal Straps: Shake Table Tests

Reyes Garcia[1*], Kypros Pilakoutas[2], Iman Hajirasouliha[3], Maurizio Guadagnini[4], Nicholas Kyriakides[5] and Mihaela Anca Ciupala[6]

Abstract

This article examines the effectiveness of two innovative retrofitting solutions at enhancing the seismic behaviour of a substandard reinforced concrete building tested on a shake table as part of the Pan-European funded project BANDIT. To simulate typical substandard construction, the reinforcement of columns and beam-column joints of the full-scale structure had inadequate detailing. An initial series of shake table tests were carried out to assess the seismic behaviour of the bare building and the effectiveness of a first retrofitting intervention using Post-Tensioned Metal Straps. After these tests, columns and joints were repaired and subsequently retrofitted using a retrofitting solution consisting of Carbon Fibre Reinforced Polymers and Post-Tensioned Metal Straps applied on opposite frames of the building. The building was then subjected to unidirectional and three-dimensional incremental seismic excitations to assess the effectiveness of the two retrofitting solutions at improving the global and local building performance. The article provides details of the above shake table testing programme and retrofitting solutions, and discusses the test results in terms of the observed damage, global damage indexes, performance levels and local strains. It is shown that whilst the original bare building was significantly damaged at a peak ground acceleration (PGA) of 0.15g, the retrofitted building resisted severe three-dimensional shake table tests up to PGA=0.60g without failure. Moreover, the retrofitting intervention enhanced the interstorey drift ratio capacity of the 1st and 2nd floors by 160% and 110%, respectively. Therefore, the proposed dual retrofitting system is proven to be very effective for improving the seismic performance of substandard buildings.

Keywords: *Shake Table Tests; Full-scale Buildings; Seismic Retrofitting; CFRP Composites; Post Tensioned Metal Straps; Substandard RC buildings*

[1] Post-Doctoral Research Associate. Dept. of Civil and Structural Engineering, The University of Sheffield, Sir Frederick Mappin Building, Mappin Street, Sheffield, S1 3JD, UK. Email (corresponding author*): r.garcia@sheffield.ac.uk.

[2] Professor. Dept. of Civil and Structural Engineering, The University of Sheffield, Sir Frederick Mappin Building, Mappin Street, Sheffield, S1 3JD, UK.

[3] Lecturer. Dept. of Civil and Structural Engineering, The University of Sheffield, Sir Frederick Mappin Building, Mappin Street, Sheffield, S1 3JD, UK.

[4] Senior Lecturer. Dept. of Civil and Structural Engineering, The University of Sheffield, Sir Frederick Mappin Building, Mappin Street, Sheffield, S1 3JD, UK.

[5] Post-Doctoral Researcher, Dept. of Civil Engineering and Geomatics, Cyprus University of Technology, 3036, Limassol, Cyprus.

[6] Senior Lecturer, School of Architecture, Computing and Engineering, University of East London, 4-6 University Way, Beckton, London, E16 2RD, UK.

1 Introduction

High human and financial losses caused by severe earthquakes (e.g. Kashmir, 2005; China, 2008; Indonesia, 2009; Haiti, 2010; Turkey, 2011; Nepal, 2015) have highlighted the high seismic vulnerability of the existing building stock, much of which comprises non-ductile reinforced concrete (RC) frame buildings built before the introduction of modern seismic design guidelines. The collapse of many of these substandard structures has been frequently attributed to failure of beam-column joints due to inadequate detailing of the joint reinforcement. Different conventional retrofitting techniques have been examined in the past to enhance the performance of substandard joints, such as concrete/shotcrete jacketing (Karayannis et al. 2008; Tsonos 2010; Corazao and Durrani 1989) or steel jacketing/steel plates (Corazao and Durrani 1989; Ghobarah et al. 1996; Biddah et al. 1997). Although the above techniques can be effective at reducing the seismic vulnerability of the current building stock, they can be highly invasive, labour intensive and they usually increase the mass of the building.

In recent years, the use of externally bonded Fibre Reinforced Polymers (FRP) has proven very effective at enhancing the seismic performance of deficient joints (e.g. Antonopoulos and Triantafillou 2003; Ghobarah and El-Amoury 2005; Pantelides and Gergely 2008; Akguzel and Pampanin 2010; Parvin et al. 2010; Al-Salloum et al. 2011; Ilki et al. 2011; Sezen 2012). In comparison to the above traditional retrofitting techniques, FRP materials have advantages such as high resistance to corrosion, excellent durability, high strength to weight ratio, and ease and speed of in-situ application (Gdoutos et al. 2000). However, the relatively high initial cost of the FRP materials may prevent its wide use. As a result, alternative retrofitting solutions combining FRP composites with other traditional techniques (e.g. steel jacketing) have been proposed (Ghobarah and El-Amoury 2005; Li et al. 2009; Sasmal et al. 2011). Such 'dual' alternatives can offer effective and attractive solutions for substandard structures, particularly in developing countries where the cost of FRP materials can be considerably higher compared to steel and local labour costs.

Previous research by Frangou et al. (1995) and Frangou (1996) led to the development of a novel technique for retrofitting RC beams and columns using Post-Tensioned Metal Straps (PTMS). The technique uses ductile

high-strength steel straps post-tensioned around RC elements using pneumatic strapping tools as those used in the packaging industry (see Fig. 1). To maintain the tensioning force after post-tensioning, the strips are fastened mechanically using jaws and push type seals. This provides active confinement to members, thus increasing their ductility and capacity before applying load. Compared to traditional steel/concrete jacketing, PTMS retrofitting has advantages such as ease and speed of application, low material cost and ease of quickly removing/replacing damaged strips and seals. As no adhesives or sophisticated equipment is used, PTMS retrofitting is also expected to provide cost-effective retrofitting solutions due to lower material and labour costs. Experimental research has confirmed the effectiveness of the PTMS technique at enhancing the capacity of columns under compression (Moghaddam et al. 2010), beams with short lap-splices (Helal et al. 2014) and substandard beam-column joints subjected to cyclic load (Helal 2012). More recently, the technique was proven extremely effective at enhancing the seismic behaviour of a full-scale PTMS-retrofitted RC building subjected to low and medium-intensity (up to PGA=0.35g) shake table tests (Garcia et al. 2014a). However, the behaviour of PTMS-retrofitted structures subjected to severe shaking (PGA>0.40g) still needs to be investigated. Moreover, the potential use of 'dual' retrofitting solutions combining FRP and other alternative techniques has not been examined using full-scale tests. The use of the 'dual' retrofitting strategy can result in more cost-effective solutions as only the weaker members of the building are retrofitted with stronger/stiffer FRP composites, whereas stronger members can be retrofitted using innovative inexpensive techniques such as the PTMS.
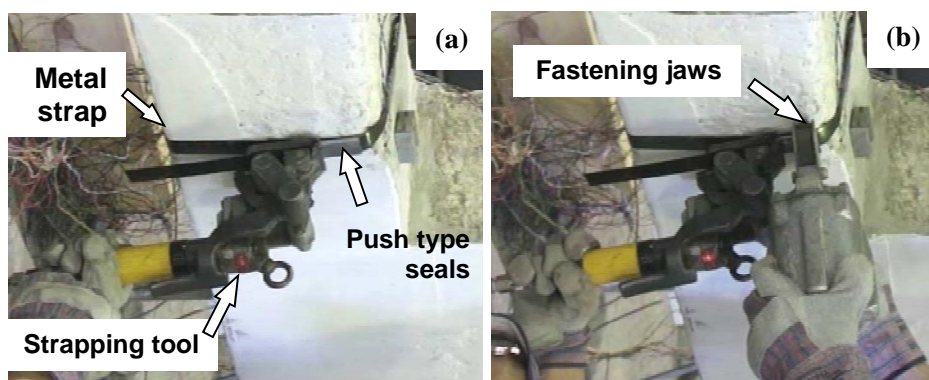

Fig. 1 (a) Post-tensioning and (b) mechanical fastening of straps around an RC member using the PTMS technique

This article investigates the effectiveness of a 'dual' retrofitting solution using Carbon Fibre Reinforced Polymers (CFRP) and PTMS at improving the performance of a previously damaged full-scale RC building with deficient beam-column joints. The structure was subjected to five Phases of shaking table tests at the CEA/EMSI laboratory facilities (Saclay, France) as part of the EU-funded BANDIT project. The initial shake table tests were reported in Garcia et al. (2014a) and investigated the behaviour of the bare (Phase 1) and PTMS-retrofitted building under low and medium-intensity shaking (Phases 2 and 3) of up to PGA=0.35g. For the first time, this article presents full details of testing Phases 4 and 5 of the project, where an innovative 'dual' retrofitting solution combining CFRP and PTMS was utilised to retrofit the building. The proposed 'dual' retrofitting solution allowed a direct comparison of the effectiveness of the two techniques using full-scale 3D shaking table tests at high PGA levels (up to PGA=0.60g). The article details the adopted retrofitting strategy, and discusses global and local results from the shake table tests on the retrofitted structure. This study is part of a comprehensive research effort focusing on the seismic retrofitting of substandard RC buildings using PTMS (Garcia et al. 2014a) and FRP composites (Garcia et al. 2014b, 2015).

2 Experimental programme

2.1 Characteristics of tested building

The geometry of the full-scale two-storey one-bay building was similar to a substandard structure tested previously by the authors (Garcia et al. 2010). The building had a regular plan of 4.26×4.26 m and a constant floor height of 3.30 m (Fig. 2a-b). The columns had a cross section of 260×260 (Fig. 2c) and longitudinal column bars of Ø14 mm (Ø is the bar diameter). These column bars were lapped over a length l_b=25Ø=350 mm just above the 1st floor joints to represent old construction practices, as shown in Fig. 2d.
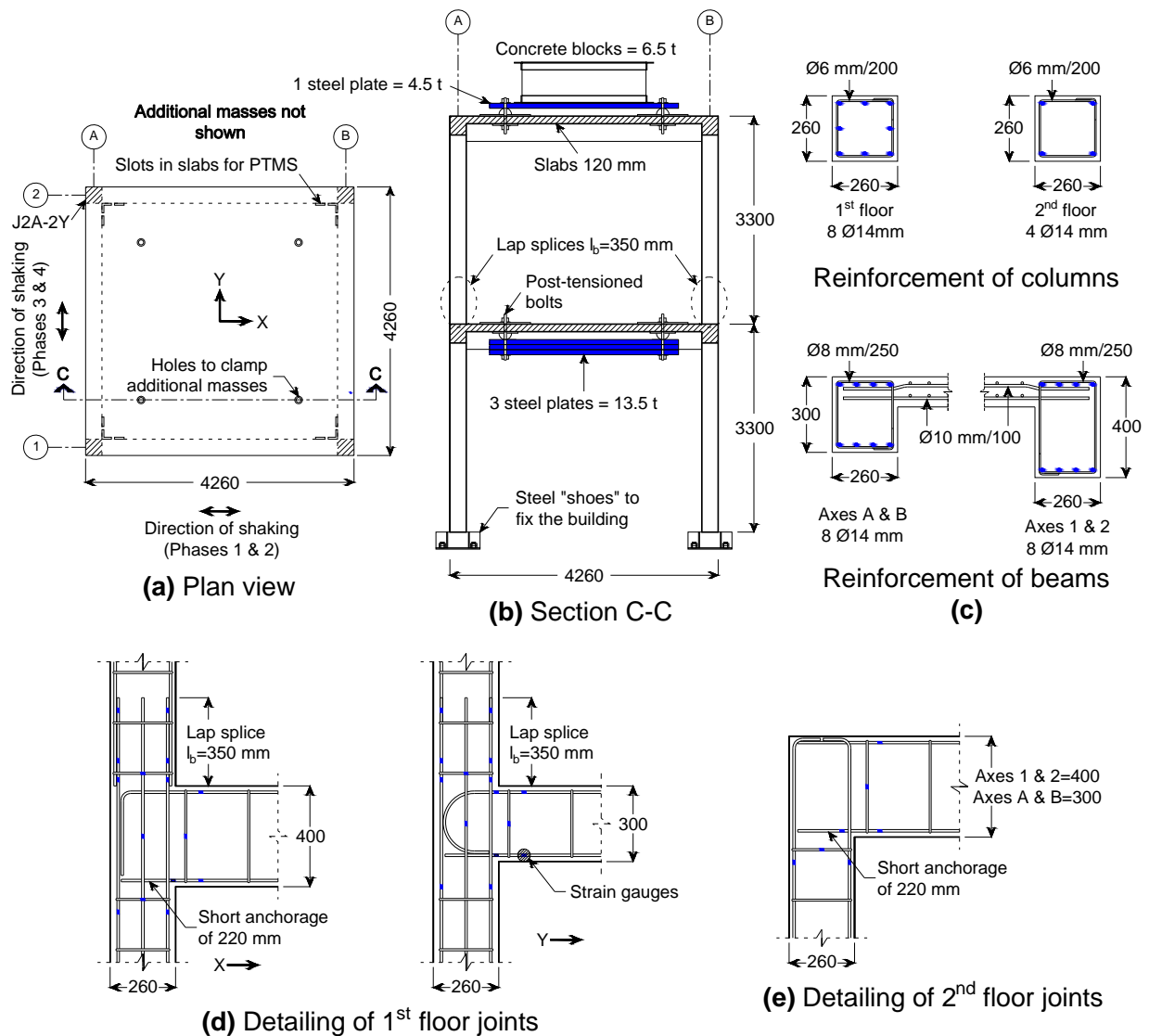
Fig. 2 General geometry and reinforcement detailing of BANDIT building (units: mm), partially adapted from Garcia et al. (2014a)

The beams had a cross section of 260×400 mm in the X direction and 260×300 mm in the Y direction (see Fig. 2c). The smaller beam depth was selected to increase the flexibility of the building in the Y direction, thus promoting large interstorey drifts (and therefore damage) in such direction during the tests at higher PGA levels. The longitudinal beam reinforcement consisted of Ø14 mm bars. The bottom beam reinforcement was anchored into the joints with no hooks/bends for a length of 220 mm (approximately 16Ø) to study the effect of deficient bar anchorage, as shown in Fig. 2d. This short anchorage length would be considered insufficient to develop the full capacity of the Ø14 mm bars according to Eurocode 2 (EC2) (CEN 2004a). The top beam

5

reinforcement of the 1st floor joints was anchored using 90° bends and U-shaped hooks, which provided adequate anchorage according to EC2 requirements. The top and bottom beam reinforcement was anchored into the 2nd floor joints for 220 mm in both X and Y directions, as shown in Fig. 2e. It should be mentioned that the beam reinforcement at the 2nd floor joints were welded to the longitudinal column reinforcement to repair the building after damage. The column-to-beam relative flexural strength ratio ($\Sigma M_{Rcol}/\Sigma M_{Rbeam}$) in the bare condition did not satisfy the strong column-weak beam strength philosophy recommended in current seismic design codes. To prevent shear failures outside the joints, the columns were reinforced with Ø6 mm stirrups spaced at 200 mm centres, whereas the beams were reinforced with Ø8 mm stirrups spaced at 250 mm centres. The stirrups were closed with 90° hooks instead of 135° hooks typically required by current seismic codes. No confining stirrups were provided in the beam-column joint cores and, therefore, significant damage was expected in these components. The top and bottom of the 120 mm thick slabs were reinforced with 10 mm bars spaced at 100 mm centres in both directions.

The columns and beam-column joints of the building were identified using an ID code according to their location in plan and elevation. The first letter of the ID represents the type of structural member ("C"=column, "J"=joint), while the subsequent digit and letter stand for the axes' intersection at which the member is located in plan. The last digit and letter indicate the floor number and the direction being considered. For instance, the element J2A-2Y corresponds to the beam-column joint of the 2nd floor located at the intersection of axes 2 and A, and parallel to the Y axis (see Fig. 2a).

2.2 Construction of specimen and material properties

The building was cast using two batches of ready-mixed normal-strength concrete, one for each floor. The 1st floor columns were cast on stiff steel "shoe" supports (see Fig. 2b), which were later clamped to the shake table using post-tensioned high-strength bolts to fix the building rigidly. Before casting, rectangular pieces of expanded polystyrene were placed at the locations shown in Fig. 2a to produce vertical slots through the slabs and ease the subsequent installation of the metal straps at beam ends. Four pieces of quarter pipes (radius=20 mm) were glued to the corners of the columns' formwork to avoid grinding the sharp corners at the retrofitting

zones. Four plastic pipes were also inserted vertically in each slab formwork to allow the clamping of additional masses (Fig. 2a-b).

After casting, each floor was cured for seven days in the formwork and then kept under standard laboratory conditions. The mean concrete compressive strength (f_{cm}) and elastic modulus of each batch were determined from tests on nine 160×320 mm concrete cylinders according to the CPC8 guidelines (RILEM 1994). The indirect tensile splitting strength (f_{ctm}) was determined from tests on twelve 160×320 mm cylinders according to EN 12390-6 (CEN 2009b). The modulus of rupture (f_{cf}) was obtained from four-point bending tests on three 100×100×500 mm prisms, according to EN 12390-5 (CEN 2009a). All specimens were cast at the same time and cured next to the building. Table 1 summarises the mean values and standard deviations obtained from the tests. It should be noted that whilst some existing substandard RC buildings were built using low-strength concrete (f_{cm}<20 MPa), it was impossible to produce such concrete using the equipment available in the testing facilities and the local (high quality) materials used by ready-mix concrete providers. Nonetheless, the strength of the concrete used in this study is representative of typical constructions built during the 1970-80s in the Middle-East, Latin America and Mediterranean regions.

Table 1 Mean mechanical characteristics of concrete mixes used to cast the building

	1st floor	2nd floor
Compressive strength, f_{cm} (MPa)	30.7 (1.56)	24.6 (2.03)
Indirect tensile strength, f_{ctm} (MPa)	2.67 (0.38)	2.28 (0.22)
Flexural strength, f_{cfm} (MPa)	3.60 (0.26)	3.83 (0.32)
Elastic modulus, E_{cm} (GPa)	24.3 (1.30)	21.2 (1.16)

Note: standard deviations shown in parentheses

Due to difficulties in finding low-strength plain bars, the building was reinforced using ribbed bars grade S500 complying with NF A 35-016-1 (AFNOR 2007). In comparison to low-strength bars, the use of such reinforcement is more critical as joints and columns can be subjected to higher force and bond demands during the tests. Table 2 summarises the mechanical characteristics obtained from direct tension tests on each bar size (three samples for each bar). Based on previous research (Helal 2012), commercially available high-strength metal straps with nominal cross section 0.8×25 mm and zinc corrosion-resistant surface coating were used for

the PTMS retrofitting. The mechanical properties of the straps were obtained from four sample coupons as reported in Table 2.

Table 2 Mean mechanical properties of steel reinforcement and metal straps

Nominal size (mm)	Ø6	Ø8	Ø10	Ø14	Strap 0.8×25 mm
Yield strength, f_y (MPa)	574 (6)	544 (12)	513 (4)	526 (8)	982 (11)
Tensile strength, f_u (MPa)	604 (9)	572 (9)	587 (9)	616 (2)	1100 (22)
Yield strain, ε_y (%)	0.28	0.26	0.25	0.26	0.43
Elongation at max. force, ε_u (%)	3.0 (0.9)	3.3 (0.6)	6.8 (1.5)	8.0 (2.3)	4.60 (0.5)
Elastic modulus, E_s (%)	207	209	202	201	230

Note: standard deviations are shown in parentheses

The bidirectional (0°-90°) CFRP sheets used for the retrofitting (see Section 2.5.2) had 70% of the fibres oriented in the main longitudinal direction of the sheets. Table 3 summarises the nominal properties of the CFRP sheets, adhesive and full composite data provided by the manufacturer.

Table 3 Mechanical properties of CFRP retrofitting system

	Tensile strength (MPa)	Elastic modulus (GPa)	Elongation at rupture (%)	Fibre thickness (mm)	Bond to concrete (MPa)
Torayca T700SC dry fibres	4900	230	2.1	0.27[b]	-
Eponal adhesive[a]	29.3 ±1.2	2.3 ±0.12	2.4 ±0.3	-	>2.5
Full composite	1350	105	1.3	0.48	-

[a] Mechanical characteristics in tension after 7 days of hardening at 23°C

[b] Thickness of 100% of the CFRP fabric

2.3 Test setup

2.3.1 Building fixity and additional masses

The building was rigidly fixed to the shake table using stiff steel "shoe" supports clamped with post-tensioned high-strength bolts. The longitudinal column reinforcement was anchored with a 90° bend welded on the base of the "shoes" to prevent failure at the column-"shoe" interface during the tests at high PGA levels. To simulate additional permanent and variable loads, three steel plates with a total mass of 13.5 tonnes were bolted beneath the 1st floor slab using post-tensioned high-strength bolts, as shown in Fig. 2b. Similarly, one steel plate and

one concrete block were clamped to the top of the 2nd floor slab to add a mass of 11.0 tonnes. These steel plates were supported on four half-ball steel bearings at the expected slab inflection points to allow free flexural deformation of the slabs during the tests. The estimated selfweight of the building was 20.4 tonnes. The selfweight and the additional masses produced approximate normalised axial load ratios $v=N/(f_cA_g)$ of 0.05 and 0.03 for the 1st and 2nd floor columns, respectively, where N is the axial load and A_g is the column gross cross sectional area. Such relatively low axial load ratios are common in many substandard low-rise RC buildings with short to medium span lengths between columns (up to 5 m).

2.3.2   Instrumentation

Fig. 3 shows the location of the horizontal displacement and acceleration transducers used to monitor the response history of each floor during the experiments. To identify possible in-plan torsion, two equidistant displacement transducers were fixed on each exterior face of the slabs. The displacement transducers were attached to a reference external rigid frame to facilitate the measurements and quantify the residual displacements after each test. Relative horizontal displacement between the slabs and the additional masses was also monitored using potentiometers. A series of 59 strategically placed electrical resistance strain gauges monitored the strain developed along the reinforcing steel of selected beams and columns at joints J2A-1X, J2A-2X, J1A-1Y, J1B-1Y and J1A-2Y (see Fig. 2d and e). In testing Phases 4 and 5, 13 additional gauges measured the strain along the metal straps and the main direction of the CFRP sheets. More information about the experimental setup is provided in Mongabure (2012).
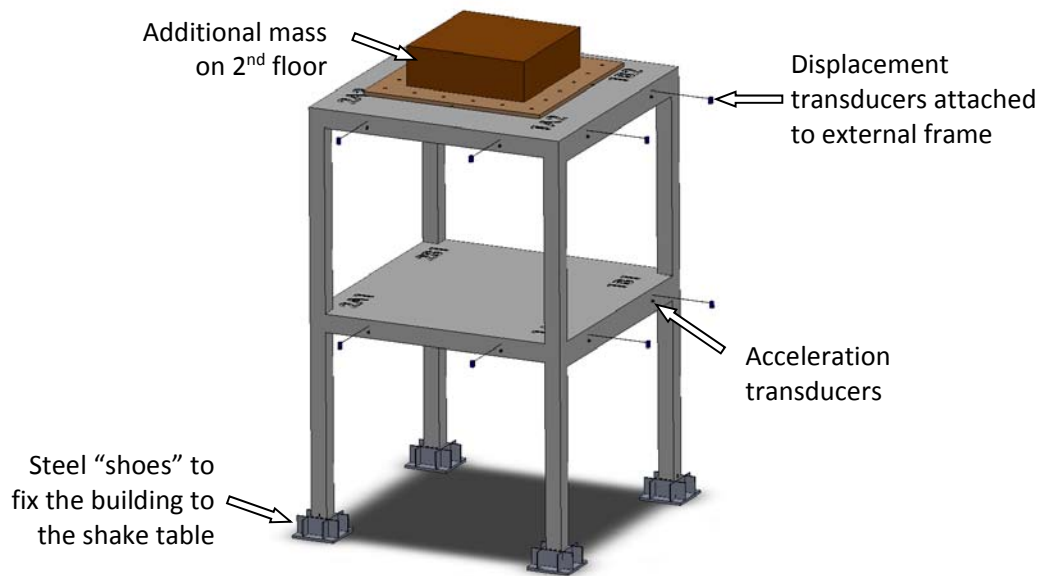
Fig. 3 Displacement and acceleration transducers used to monitor the building response

2.3.3 Test sequence

The full testing programme consisted of 30 shaking table tests conducted in five phases according to the sequence summarised in Table 4. Phase 1 of the experiments consisted of shake table excitations in the X direction (i.e. parallel to axes 1 and 2 in Fig. 2a) up to a maximum PGA=0.15g. The main objective of these tests was to investigate the seismic performance of the substandard RC structure and produce significant, but repairable damage. The effectiveness of the PTMS retrofitting technique was then investigated in Phases 2 (X direction) and 3 (Y direction) of the project, but the shaking table tests were halted at a PGA level of 0.35g to visually assess damage in the building. To compare the performance of the two retrofitting solutions using CFRP and PTMS, testing Phase 4 subjected the building to input records in the Y direction, i.e. parallel to frames A and B in Fig. 2a. Finally, the tests in Phase 5 allowed investigating the behaviour of the retrofitted building under severe 3D shaking.

Table 4 Full test sequence of BANDIT building and dynamic properties after each test, partially adapted from Garcia et al. (2014a)

Phase	Test direction and condition	PGA (g)	X direction		Y direction	
			1st mode T_1 (s)	2nd mode T_2 (s)	1st mode T_1 (s)	2nd mode T_2 (s)
1	X - Bare building	Undamaged	0.48[b]	0.18	0.52[b]	NA
		0.025	0.53	0.20	-	-
		0.05	0.60	0.22	-	-
		0.10	0.68	0.25	-	-
		0.15[a]	0.88	0.29	-	-
2	X - Repaired and PTMS-retrofitted building	Initial	0.61	0.20	0.65	NA
		0.05	0.64	0.21	-	-
		0.10	0.67	0.22	-	-
		0.15	0.68	0.23	-	-
		0.20	0.75	0.23	-	-
		0.25	0.78	0.26	-	-
		0.30	0.88	0.26	-	-
		0.35	1.01	0.27	-	-
3	Y - PTMS-retrofitted building R_Y	Damaged	-	-	0.84	0.27
		0.05	-	-	0.86	0.27
		0.10	-	-	0.93	0.27
		0.15	-	-	0.93	0.28
		0.20	-	-	0.97	0.29
		0.25	-	-	1.08	0.29
		0.30[a]	-	-	1.11	0.30
4	Y - Repaired, CFRP/PTMS-retrofitted R_Y	Initial	0.75	0.23	0.84	0.25
		0.05	-	-	0.88	0.25
		0.10	-	-	0.93	0.27
		0.20	-	-	0.99	0.28
		0.30	-	-	1.03	0.29
		0.35	-	-	1.09	0.30
5	XY - CFRP/PTMS-retrofitted XYZ - CFRP/PTMS-retrofitted $R_Y+0.85R_X+0.5R_Z$	0.10	0.95	0.27	1.09	0.30
		0.10	0.99	0.28	1.20	0.31
		0.20	0.97	0.29	1.20	0.31
		0.30	0.97	0.29	1.20	0.31
		0.35	1.08	0.30	1.20	0.31
		0.40	1.06	0.31	1.20	0.32
		0.50	1.22	0.32	1.22	0.33
		0.60	1.22	0.32	1.37	0.34

[a] After this test, cracks were resin-injected and damaged concrete replaced with high-strength epoxy mortar

[b] T_{iX}=0.48 s; T_{iY}=0.52 s

2.3.4 Seismic records and dynamic identification

A 30 seconds-long artificial ground motion record based on Eurocode 8 (EC8) soil type C spectra (EN 1998-1:2004, CEN 2004b) was used as horizontal input signal during Phase 4 (see record R_Y in Table 4). The ground motion record was scaled to apply different levels of peak ground acceleration (PGA). In Phase 5, two additional records based on EC8 were used as input in the lateral X (record R_X in Table 4) and vertical (record R_Z) directions to apply 3D shaking. However, the PGAs of the input records in the X and vertical directions were scaled down to 85% and 50% of the total in Y direction, respectively (see Table 4). Note that the 85% scaling is consistent with observations from strong ground motion data (Clough and Penzien 2003) and is suggested for 2D/3D testing by international codes such as the Chinese Seismic Code GB50011-2001 (2001). The vertical record is scaled down by 50% to consider a ratio of vertical to horizontal (Y) accelerations (a_{vg}/a_g) of 0.50, which is only slightly larger than the value a_{vg}/a_g=0.45 suggested by EC8.

In general, a good matching between the input record spectra and the shake table response spectra was observed for the range of frequencies of interest at all excitation levels. For instance, Fig. 4 compares the spectra for the "EC8" for 5% of critical damping, the "input" record, and the actual response recorded on the "Azalée" shake table at PGA=0.30g. It is shown that the input record spectra matched well the table response spectra of EC8.
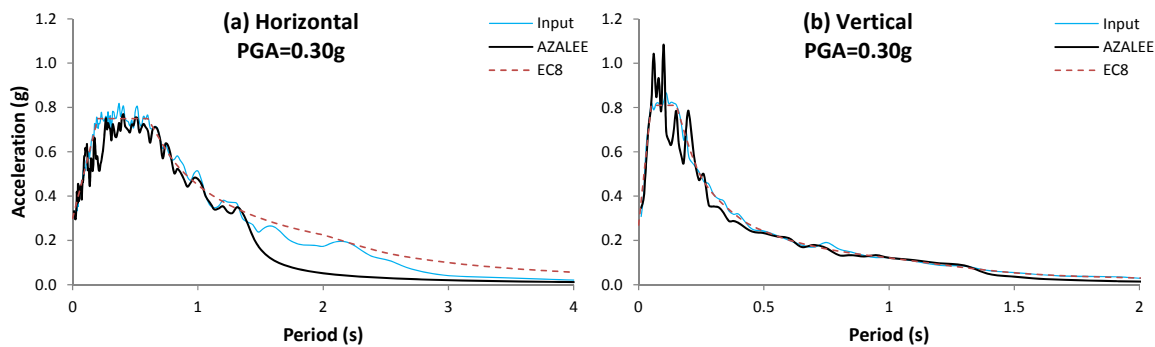
Fig. 4 Matching of input records in (a) horizontal and (b) vertical directions with shake table response and EC8 spectra (PGA=0.30g)

Natural frequencies of the structure were determined before and after each test using a low intensity white noise excitation (maximum PGA=0.05g) containing a frequency range of 0.5-50 Hz. The response recorded at each floor was then used to identify the natural frequencies of the relevant vibration modes. Accordingly, Table 4

24   reports the structural periods of the fundamental (T_1) and second (T_2) vibration modes of the building at the

25   different testing phases. All data were collected by a data acquisition system at a sampling frequency of 600

26   Hz during 50 seconds.

27   ### *2.4   Summary of testing Phases 1 to 3*

28   The seismic performance of the RC building was initially investigated through a series of unidirectional shake

29   table tests in two orthogonal directions, as reported in Garcia et al. (2014a). Seismic tests were first performed

30   in the X direction of the bare building (Phase 1). The tests were halted at a PGA=0.15g to avoid a possible

31   collapse of the 2nd floor caused by the premature local failure of the beam-column joints. Such failure was

32   expected due to the short anchorage of the longitudinal beam reinforcement, as shown in Fig. 2e. Subsequently,

33   the damaged concrete at the joints was repaired using high-strength epoxy mortar, the main cracks were epoxy-

34   injected, and the joints and columns were retrofitted using the PTMS technique as shown later in Section 2.5.3.

35   In testing Phases 2 and 3, the PTMS-retrofitted building was subjected to shaking in the X and Y directions,

36   respectively. The building sustained medium-intensity earthquakes up to a PGA=0.35g and maximum

37   interstorey drift ratios δ=2.80% at the 2nd floor. This implies that the structure remained within the Collapse

38   Prevention (CP) performance level according to ASCE/SEI 41-06 (ASCE 2007) (i.e δ<4.0%) without risking

39   stability. Readings from strain gauges on the longitudinal bars of beam-column joints indicated that the

40   reinforcement remained within the elastic limits during testing Phases 1-3. A visual inspection after testing

41   Phase 3 indicated that the retrofitted building was clearly capable of sustaining seismic excitations at higher

42   PGA levels as the majority of the straps maintained their post-tensioning force. However, the tests were halted

43   to evaluate the local damage at the joints and assess the global condition of the structure.

44   ### *2.5   Repairs and seismic retrofitting - Phases 4 and 5*

45   #### **2.5.1   Crack injection and concrete patching**

46   After testing Phase 3, the removal of the metal straps and spalled concrete revealed considerable damage in the

47   1st and 2nd floor joints, as shown in Fig. 5a-b. Therefore, the damaged joints were repaired for a second time.

48   Firstly, the external top and bottom longitudinal beam bars (with an anchored length of 220 mm only) were

49   exposed and welded to the column bars to prevent a possible bar pullout in the 2nd floor joints. To achieve this,

50 some concrete was removed from the joints in the Y direction and the bars were welded together using single

51 "points" of welding, as shown in Fig. 5c. Although pullout failure of bars was not observed during testing

52 Phases 2 and 3, the welding was carried out to prevent a possible collapse of the 2nd floor during the tests at

53 higher PGA intensities. In real buildings, such welding would be necessary to prevent pullout of the straight

54 longitudinal beam bars if the joints were detailed as shown in Fig. 2e. Damaged and spalled concrete was

55 replaced with high-strength epoxy mortar, and wide cracks were epoxy-injected as shown in Fig. 5d. After the

56 mortar and resin set, the structure was retrofitted with CFRP sheets and PTMS on two opposite frames as

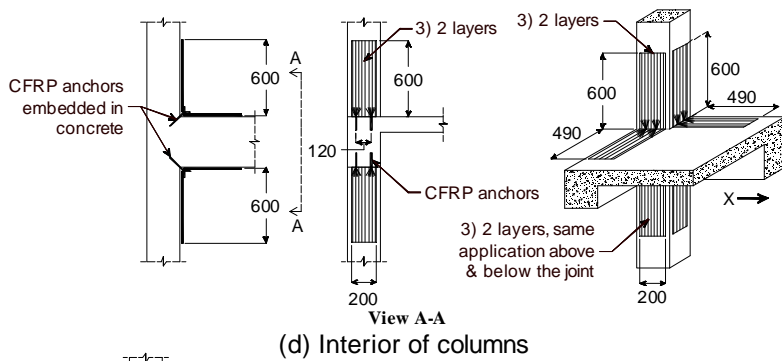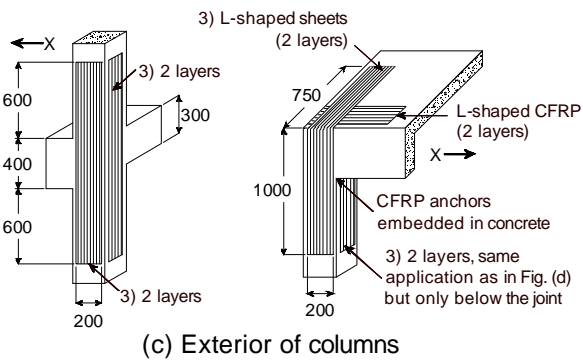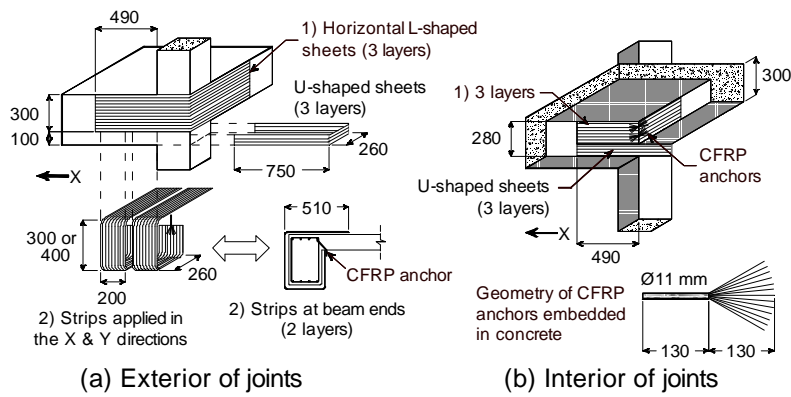57 described in the following section.

58

59
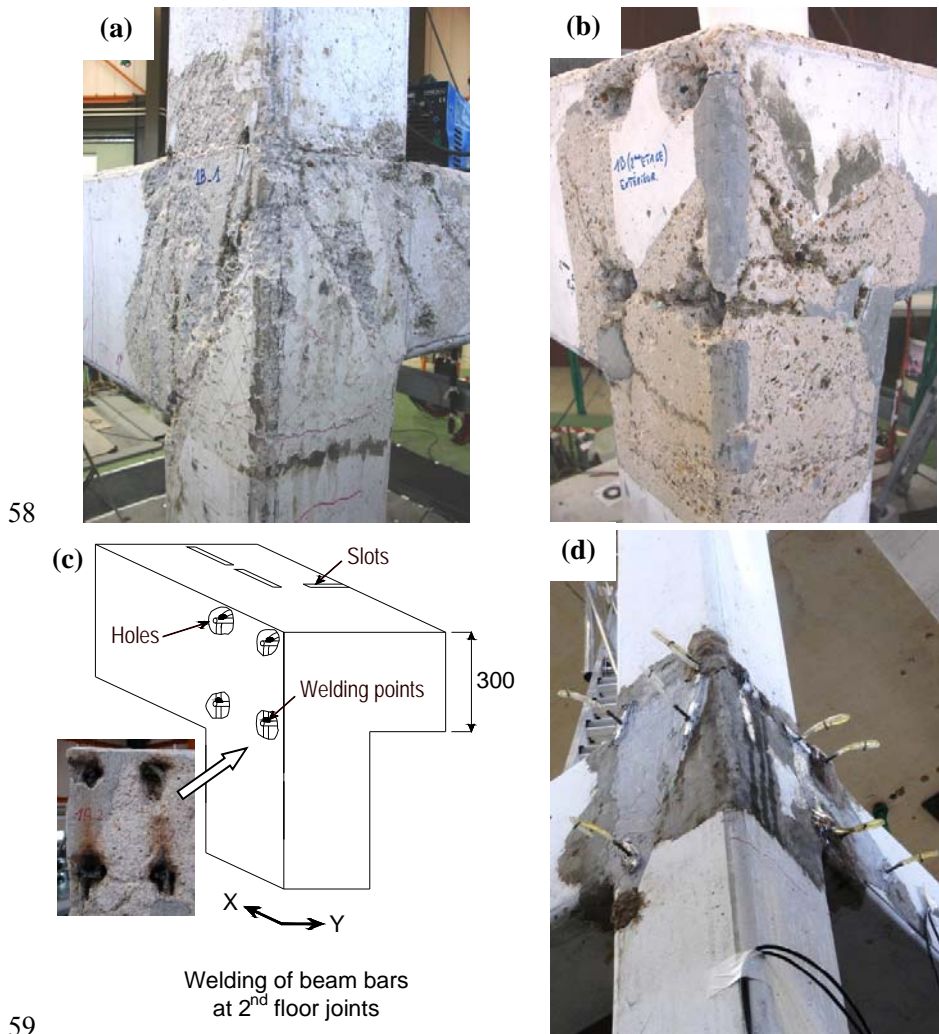
60 **Fig. 5** Observed damage after removal of PTMS in Phase 3 (a) joint J1B-1 and (b) joint J1B-2; (c) welding of longitudinal
61 beam reinforcement to column bars; (d) view of resin injection and concrete patching at joints

62 **2.5.2   CFRP composites**

63 The dual retrofitting intervention aimed to provide a strong column-weak beam mechanism by preventing the

64 premature failure of the joints and by enhancing the flexural capacity of the columns, thus complying with

65 current seismic design philosophy. Fig. 6 shows a general view of the CFRP retrofitting solution used for frame

66 A of the building. The layout and number of CFRP sheets was similar to that used to retrofit substandard beam-

67 column joints and a full-scale building tested previously by the authors (Garcia et al. 2010; Garcia et al. 2014c).

68 Before bonding the CFRP sheets using a wet lay-up procedure, the concrete surfaces were wire brushed and

69 cleaned with pressurised air to enhance adherence. Primer resin was applied at the retrofitting zones to seal the

70 concrete surface. The CFRP sheets were fixed according to the following sequence (see Fig. 6):

15

(a) Exterior of joints

(b) Interior of joints

(c) Exterior of columns

(d) Interior of columns

(e) Confinement of columns
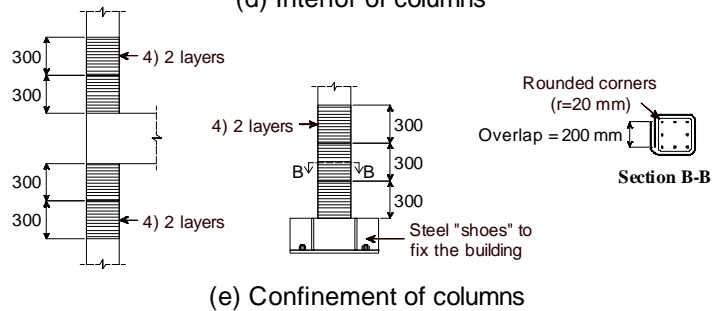
71

72 **Fig. 6** Sequence of CFRP retrofitting adopted for frame A (units: mm)

73   1) The beam-column joints were first retrofitted using horizontal L-shaped CFRP sheets (3 layers) as shown in

74   Fig. 6a. The three CFRP layers were also bonded to the interior faces of the joints. To prevent premature

75   debonding at the corners, these sheets were anchored mechanically using two CFRP anchors inserted into

76   predrilled holes at the locations shown in Fig. 6b. These anchors were designed to resist the theoretical nominal

77   tensile strength of the fibre sheets.

78   2) Next, two CFRP strips of 200 mm width (2 layers) were wrapped around the beams' ends to prevent

79   premature debonding of the horizontal sheets applied to retrofit the joints (see Fig. 6a). One end of the sheets

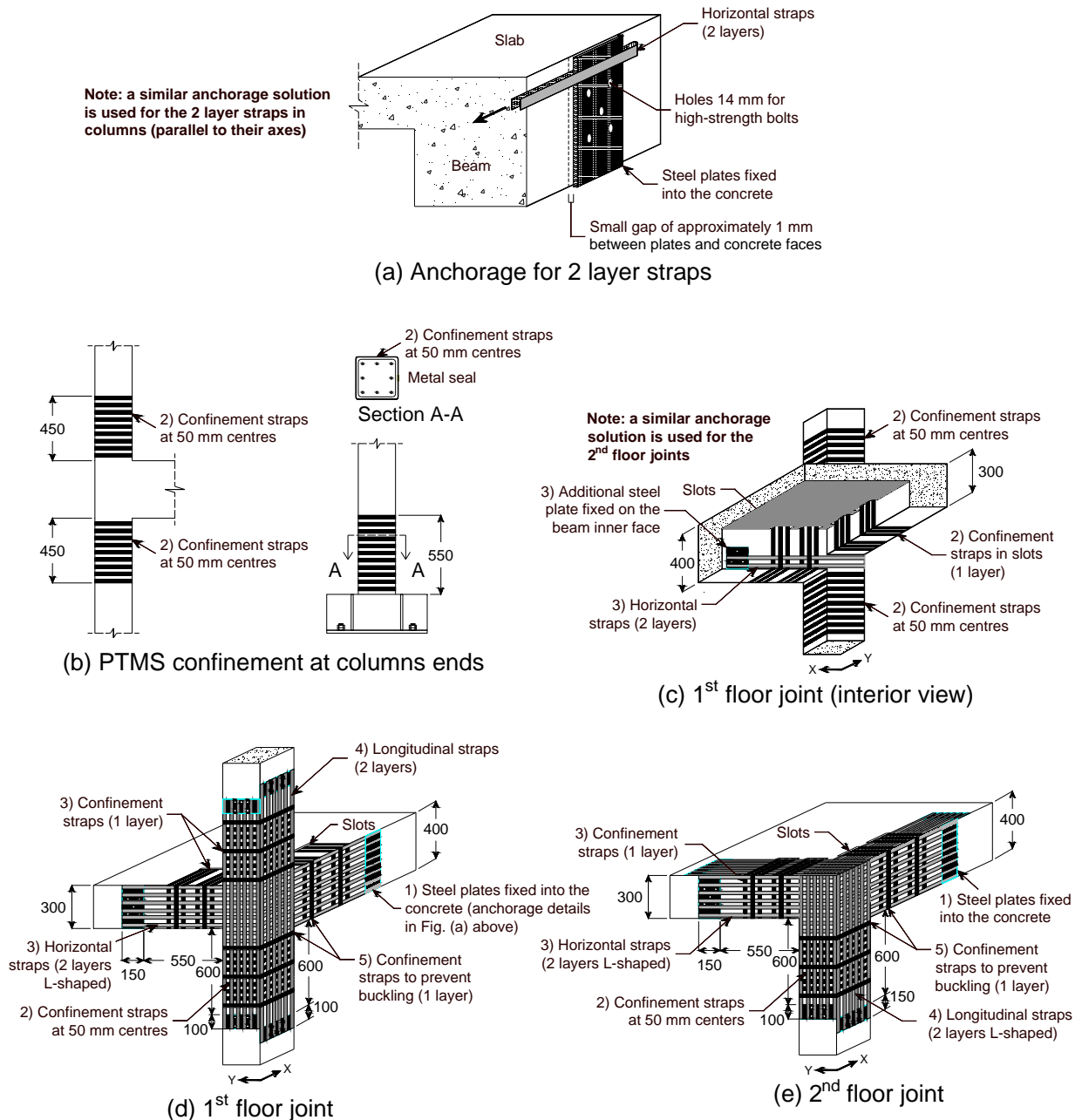80   was anchored mechanically to the bottom of the slab using a CFRP anchor.

81   3) Vertical CFRP sheets (2 layers) were bonded to the exterior (Fig. 6c) and interior (Fig. 6d) faces of the

82   columns' ends to enhance their flexural strength. This resulted in a modest flexural reinforcement ratio

83   ρ=0.32% used for the retrofitting. The interior sheets were held using two CFRP anchors (Fig. 6d) to give

84   continuity to the sheets and to avoid drilling slots through the concrete slabs.

85   4) Finally, the column ends were confined (2 layers) to avoid premature debonding of the longitudinal sheets

86   along the columns axes (Fig. 6e), and to prevent lap splice failures at the bottom of the 2nd floor columns. This

87   led to effective confinement ratios $\alpha\omega_w$ of 0.152 and 0.189 for the 1st and 2nd floor columns, respectively, where

88   α is the confinement effectiveness factor and ω_w is the volumetric mechanical ratio defined by EC8. As the

89   existing transverse reinforcement was sufficient to prevent shear failure in beams and columns, no additional

90   CFRP reinforcement was provided to prevent this type of failure.

91   **2.5.3   Post-Tensioned Metal Strapping**

92   Fig. 7 shows the PTMS retrofitting strategy adopted for frame B. The amount and layout of metal straps is

93   based on the principle that metal straps are treated as conventional tensile reinforcement, and can be designed

94   according to the procedure outlined in Garcia et al. (2014a). The straps were post-tensioned to approximately

95   30-40% of their yield strength based on previous experience from tests on columns (Frangou et al. 1995;

96   Moghaddam et al. 2010), and on substandard full-scale joint subassemblies retrofitted with PTMS (Helal 2012).

97   To ensure such post-tensioning force, the tensioning tool was pre-calibrated by applying different levels of air

98 pressure, while monitoring the effective strap force after fastening the push type seals, using a double pulley

99 setup mounted on a universal testing machine. The metal straps were installed according to the following

100 sequence (see Fig. 7):

(a) Anchorage for 2 layer straps

(b) PTMS confinement at columns ends

(c) 1st floor joint (interior view)

(d) 1st floor joint

(e) 2nd floor joint

101

102 **Fig. 7** Sequence of PTMS retrofitting adopted for frame B, partially adapted from Garcia et al. (2014a) (units: mm)

103 1) Six 10 mm thick anchor steel plates were fixed to the columns, beams and top of 2nd floor slab using high-

104 strength 12×120 mm bolts inserted in holes prefilled with epoxy adhesive mortar. After the adhesive set, the

18

plates were positioned and partially tightened with nuts and washers leaving a small gap of approximately 1 mm between the plates and the concrete faces, which was necessary to secure the 2 layer of metal straps (see Fig. 7a). For practical purposes, the steel plates were staggered to prevent congestion of the steel bolts at a single beam or column section. The sharp corners of the anchoring plates in contact with the metal straps were rounded off to a ratio of 5 mm to reduce stress concentrations and possible strap rupture. The diameter of the high-strength bolts and dimensions of the steel plates were designed to resist the shear force corresponding to the nominal tensile strength of the metal straps.

2) Next, horizontal straps at 50 mm spacing were placed at the columns ends (see Fig. 7b) to provide confinement and increase their shear strength, thus resulting in $\alpha\omega_w$=0.054 and 0.067 the 1st floor and 2nd floor columns, respectively (i.e. approximately 1/3 of the confinement applied on the CFRP-retrofitted frame). Additionally, one layer of straps was inserted in the pre-formed slots of the slabs to confine the beams ends and also increase their shear capacity (Fig. 7c).

3) Eight straps (2 layers each) were installed parallel to the longitudinal beams axes (i.e. horizontally) at 50 mm centres to provide confinement to the beam-column joint. These straps were anchored around the steel plates as shown in Fig. 7d-e. Due to the different beam depths in the X and Y directions, two of these straps were anchored using an additional anchorage plate at the interior face of the deeper beams, as shown in Fig. 7c.

4) Six straps (2 layers each) were provided along the exterior faces of the columns to enhance their flexural capacity, which lead to a retrofitting flexural reinforcement ratio ρ=0.38% parallel to the columns' axis. For the 2nd floor joints, the six straps were bent at 90° at the slab edges and secured to steel plates located on the top of the 2nd floor slab. Subsequently, the nuts of the bolts securing the steel plates were tightened by hand using a spanner to prevent the loss of tension force in the straps (Fig. 7d-e). The longitudinal column straps were curtailed at a distance of 600 mm from the beams (see Fig. 7d-e), where the column flexural strength was sufficient to resist the seismic demand.

129   5) Finally, 1 layer of confinement straps was placed around beams and columns to prevent excessive buckling

130   of the horizontal and longitudinal straps installed during steps 3 and 4 (Fig. 7d-e).

131   All straps were fastened using mild-steel push type seals of 25 mm length. Such seals are typically used in the

132   packaging industry due to their low cost and ease of installation using common strapping tools. As shown in

133   Fig. 8, the tensioning force was maintained mechanically with notches produced using the clamping jaws (four

134   notches per metal seal). As shown in the video (Online Resource 1), the installation of the metal straps was

135   performed swiftly without the need of using heavy equipment or sophisticated safety gear.
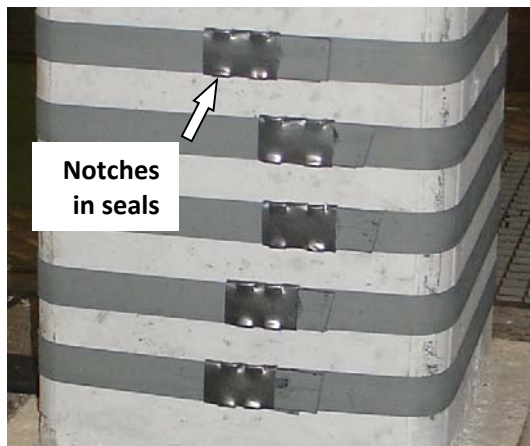
136

137   **Fig. 8** Close up view of metal seals after fastening

138   Table 5 summarises the flexural strength of beams and columns of the bare and retrofitted building for the X

139   direction. It is shown that the PTMS and CFRP retrofitting solutions increased the flexural strength of beams

140   and columns by minimum 30% to comply with the strength hierarchy in code-compliant joints imposed by EC8

141   (i.e. $\Sigma M_{Rcol} > 1.3 \Sigma M_{Rbeam}$). It should be noted that the values in Table 5 were calculated using conventional

142   moment-curvature analysis assuming 1) no post-tensioning losses in the metal straps, 2) perfect bond between

143   CFRP sheets and concrete, and 3) that the straight beam reinforcement did not pullout from the joint, as

144   confirmed during the tests in the retrofitted condition (see next section).

145 **Table 5** Beam and column flexural strengths of BANDIT building

	Bare condition		PTMS-retrofitted		CFRP-retrofitted	
	M_y	M_u	M_y	$M_u{}^{(b)}$	M_y	$M_u{}^{(b)}$
Column 2nd floor	38	41	92	102	51	83
Column 1st floor	63	77	101	119	77	105
Beams X direction (positive)	79	88	149	172	93	182
Beams X direction (negative)[a]	108	113	188	208	123	169

[a] The effective tension flange was computed according to Eurocode 2 (CEN 2004a)

[b] Values at concrete crushing

146 Fig. 9 shows the building after the retrofitting intervention. As shown in Fig. 9a, the metal strapping provided

147 a confining grid around the beam-column joints and columns ends, whereas the CFRP sheets covered

148 completely the beam-column connection (Fig. 9c).
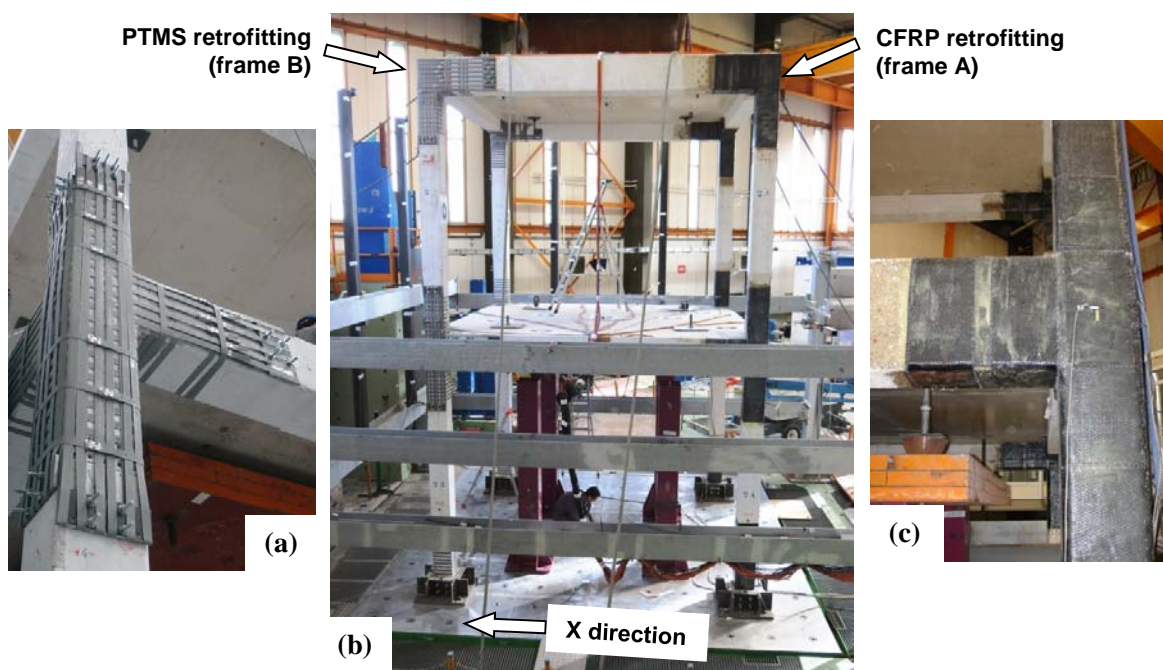
150 **Fig. 9** View of the building after the CFRP/PTMS retrofitting: (a) PTMS-retrofitted joint; (b) general view on shaking
151 table, and (c) CFRP-retrofitted joint

## 3   Test results and discussion

3.1   Phase 4: tests in Y direction

154 The seismic excitation applied to the building after the repairs and dual CFRP/PTMS retrofitting ranged from

155 PGA 0.05g to 0.35g (see Table 4). In general, as the CFRP sheets and metal straps covered the concrete

surfaces, damage at the joints could not be observed during the tests. However, popping and metallic sounds during tests (especially after the test at PGA=0.20g) indicated that the CFRP and metal straps were effectively carrying considerable tension forces. After the tests were halted, a visual inspection revealed that no apparent damage was caused on the straps or on the CFRP sheets. Overall, the metal straps maintained most of the post-tensioning force, with the exception of some longitudinal straps placed along the columns of the 1st floor joints. This loss of force can be attributed to the partial shearing off of some push type metal seals, which had poor bearing resistance to start with. Some cracking was also evident at the beam-column joints, but only on frame B where the PTMS retrofitting was applied. The damage observed in the building in Phase 4 indicated that the repairs and CFRP/PTMS retrofitting intervention prevented the premature shear failure of the deficient joints.

As the tested building is low-rise, symmetric and regular in plan and elevation, the first mode is expected to dominate the structural response (e.g. Thermou and Pantazopoulou (2011)). Therefore, this study adopts an equivalent SDOF model to calculate the global lateral stiffness of the structure (K) during testing Phase 4. Fig. 10 shows that the repairs and retrofitting restored the stiffness of the building from K=1430 kN/m (end of Phase 3) to 2510 kN/m (beginning of Phase 4), i.e. an enhancement of 75%. At the end of Phase 4 (PGA=0.35g), damage accumulation degraded the stiffness of the original bare building by 77% (from 6600 kN/m at the beginning of Phase 1 to 1500 kN/m). Despite this severe stiffness reduction, the limited structural damage observed after Phase 4 indicated that the building was capable of sustaining seismic shaking at higher intensities.
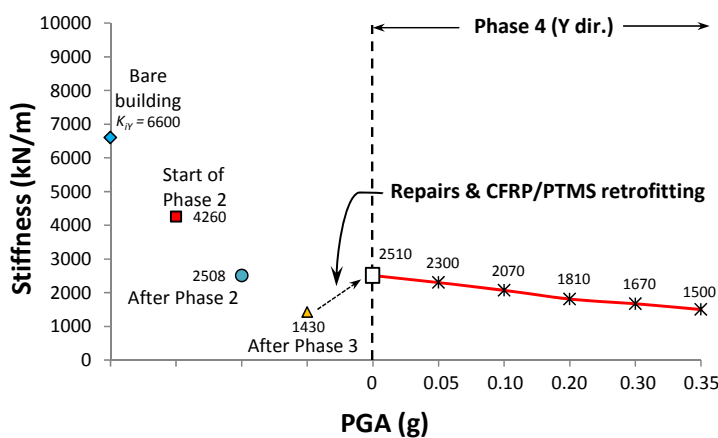

Fig. 10 Evolution of lateral stiffness during testing Phase 4 (Y direction)

3.2 Phase 5: 3D tests

176 The seismic excitation applied to the building ranged from PGA 0.10g to 0.60g (Table 4). As for Phase 4,

178 damage at the joints could not be observed during the tests. However, popping and metallic sounds after the

179 test at PGA=0.35g indicated that the CFRP sheets and metal straps were carrying considerable tension forces.

180 At PGA=0.40g, several of the push type metal seals sheared off (especially at the joints), thus leading to partial

181 loss of the post-tensioning force in the straps.

182 During the last tests at PGA=0.50g and 0.60g, some of the high-strength bolts used to fix the steel plates into

183 the 2nd floor columns bent due to the excessive shearing force applied by the metal straps. This was

184 accompanied by the opening of a gap between some of the anchoring plates and the column faces (similar to

185 that shown in Fig. 7a), leading to further loss of tension force in the straps. A visual inspection after the tests

186 revealed some horizontal cracking and concrete crushing at the base of the 2nd floor columns of frame B (see

187 Fig. 11a). Moreover, some of the concrete cover spalled off in the Y direction of column C1B-2Y (Fig. 11b)

188 probably due to the high pulling force applied by the plate and bolts. Whilst some metal seals and high-strength

189 bolts experienced minor local damage during this test Phase, frame B maintained its stability at high seismic

190 excitation levels. Based on these experimental observations, it is evident that the anchoring system was

191 effective to prevent failure of the strapping intervention. Nonetheless, further research is necessary to

192 investigate the effectiveness of the anchoring system on low-strength concrete, where the anchoring bolts may

193 cause damage to the surrounding concrete.

(a) Horizontal crack at column base

**(b)** Diagonal crack and spalled concrete cover

194
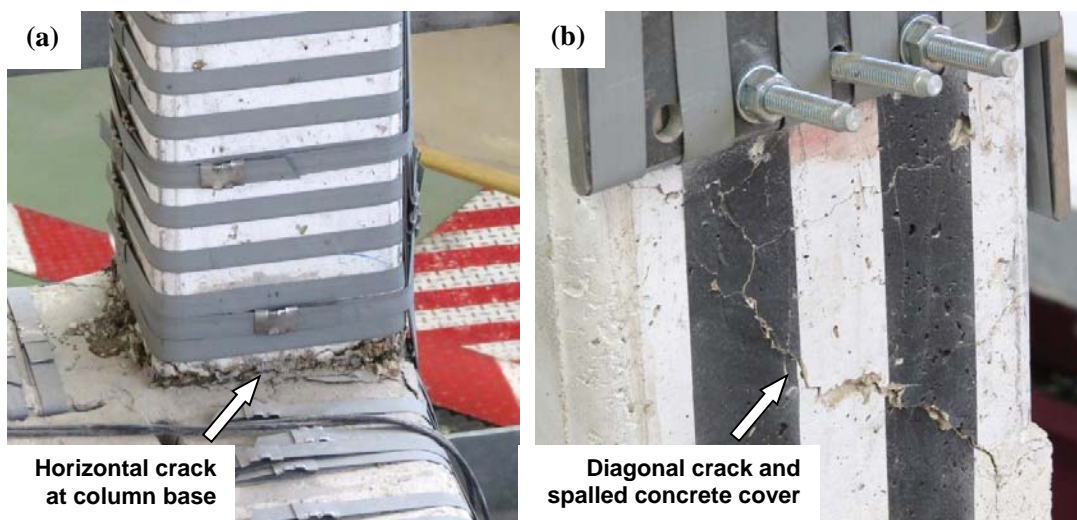
195 **Fig. 11** (a) Typical horizontal crack at the base of the 2nd floor columns of frame B; (b) diagonal crack and spalled concrete
196 cover in column C1B-2Y (Y direction)

197 A post-test visual inspection and video recordings (Online Resource 2) also indicated that horizontal cracks as

198 that shown in Fig. 11a also formed at the base of the 2nd floor columns of frame A. This was confirmed by

199 minor local debonding of some vertical CFRP sheets (see Fig. 12a) during the final seismic test at PGA=0.60g.

200 However, the crack opening was controlled by the CFRP anchors embedded at the inner faces of the columns

201 (see Fig. 6b). Minor debonding and CFRP fracture was also observed at some locations of the beam-column

202 joints (Fig. 12b-c).
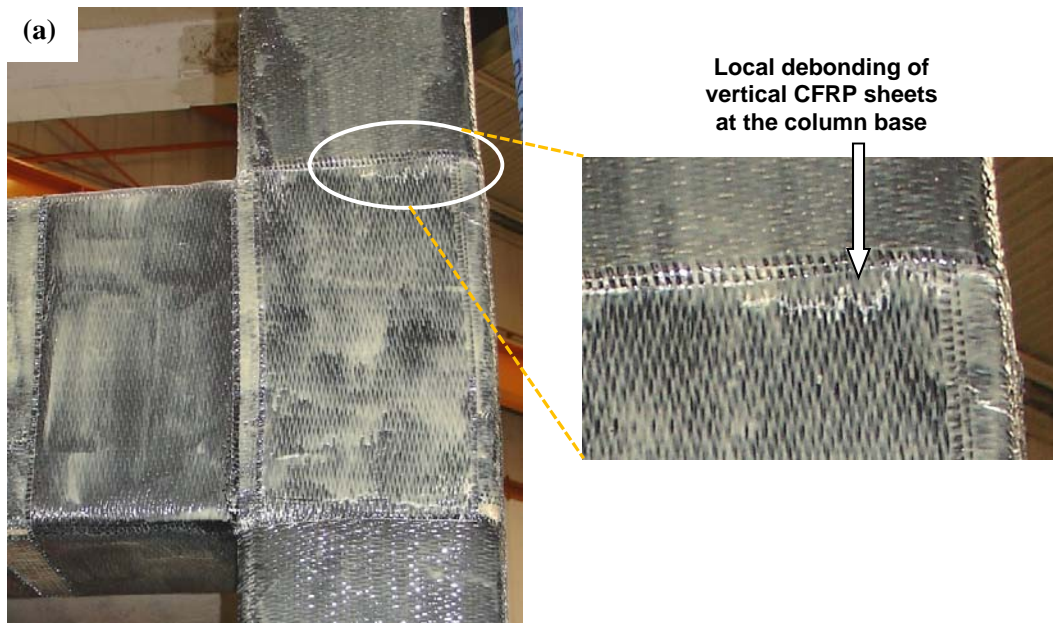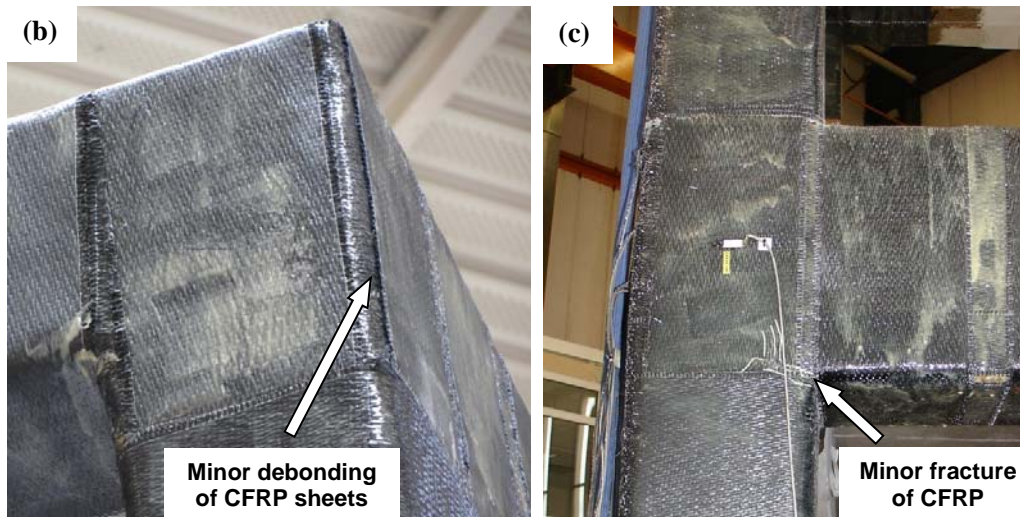
**Fig. 12** (a) Local debonding of vertical CFRP sheets at the base of column J2A-1X; (b) minor debonding at 2nd floor joints; and (c) minor fracture of CFRP sheets at joint J1A-1X

The 3D shake table tests performed in Phase 5 did not compromise the structural stability of the CFRP/PTMS-retrofitted building. Whilst it was clear that the building was capable of resisting tests at higher PGAs, the tests had to be halted after a PGA=0.60g because the maximum displacement limits of the shake table in the X and Y directions (±125 mm) were reached. It should be also mentioned that the maximum relative displacement between the additional masses and slabs was 2.1 mm at PGA=0.60g, thus confirming that the additional masses were clamped rigidly to the concrete slabs.

214   Fig. 13a-b show the lateral stiffness degradation in the X and Y directions, respectively. Compared to the

215   stiffness observed in the Y direction after Phase 4 (1500 kN/m), the stiffness after the first test of Phase 5

216   degraded by 19% (1220 kN/m). The results also indicate that the lateral stiffness in the X direction deteriorated

217   at a faster rate (from 1950 after Phase 4 to 1190 kN/m) in comparison to the Y direction. This can be attributed

218   to the damage produced in the Y direction in Phase 4. At the end of the test programme, the residual stiffness

219   of the building in both the X and Y directions was only 15% of the original stiffness (see K_{iX} and K_{iY} values in

220   Fig. 13a-b).
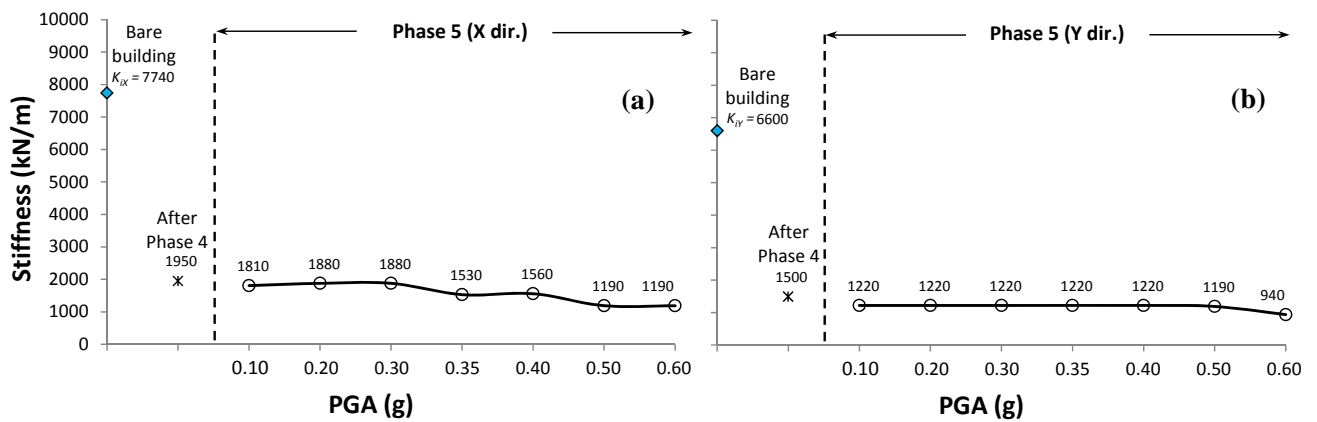
221

222   **Fig. 13** Evolution of lateral stiffness during testing Phase 5 in the (a) X and (b) Y directions
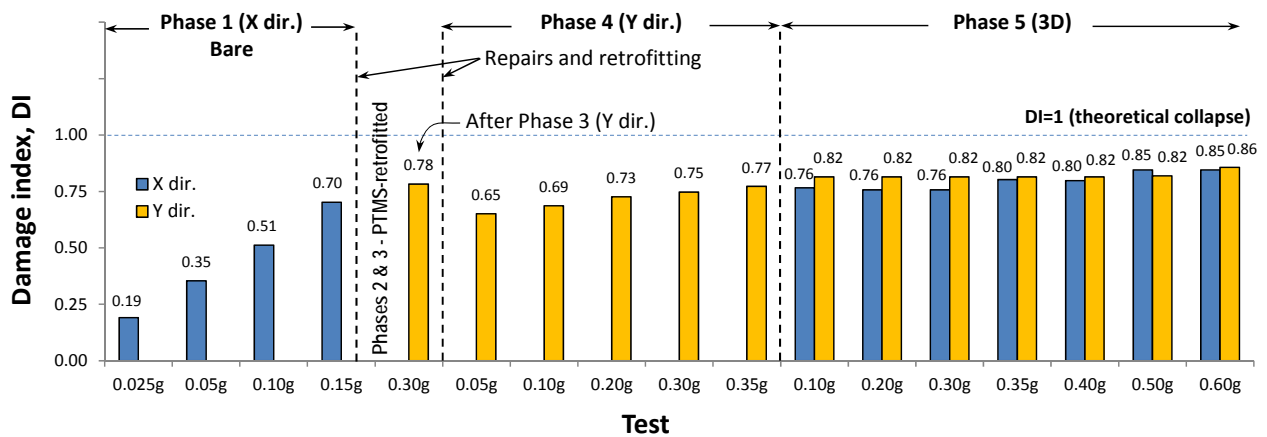
3.3 Global damage index

224   Research has suggested that the progression of global damage in buildings subjected to earthquakes can be

225   evaluated using the shift in fundamental structural period (DiPasquale et al. 1990; Zembaty et al. 2006;

226   Kyriakides et al. 2014). Therefore, this study adopts the global damage index (*DI*) developed by DiPasquale et

227   al. (1990) to assess quantitatively the progress of structural damage at different PGA intensities, as defined by

228   Equation (1):

$$DI = 1 - \left(\frac{T_i}{T_f} \right)^2 \qquad (1)$$

229   where T_i and T_f are the natural periods of the building in initial (undamaged) condition and after an earthquake,

230   respectively. Accordingly, *DI*=0 implies no damage to the building, whereas *DI*≈1.0 represents theoretical

231   building 'collapse'. Fig. 14 shows the global *DI*s calculated for each shake table test using Equation (1). For

232   each direction of testing, T_i was taken as the initial period of the bare undamaged building in that direction

233   (T_{iX}=0.48 s and T_{iY}=0.52 s), whereas T_f was taken as the period after each shake table test as summarised in

234   Table 4. It should be noted that any global damage index has to be calibrated with test and field data before it

235   can be directly associated to a specific damage state or performance limit. Therefore, the *DI* proposed by

236   DiPasquale et al. (1990) is used in this study only to compare quantitatively the progression of global structural

237   damage experienced by the building during testing Phases 1, 4 and 5.

238

239   **Fig. 14** Global damage index (Phases 1, 4 and 5), partially adapted from Garcia et al. (2014a)

240   Fig. 14 indicates that at a PGA=0.05g, the *DI* of the CFRP/PTMS-retrofitted building was 0.65, which implies

241   that the applied repairs and retrofitting reduced damage by 17% with reference to the last test of Phase 3

242   (*DI*=0.78 in the Y direction). Overall, the evolution of damage during Phase 4 was gradual, which agrees well

243   with the experimental observations. At the end of Phase 4 at PGA=0.35g, the global damage (*DI*=0.77) was

244   similar to that observed at the end of Phase 3 but at a lower PGA=0.30g (*DI*=0.78). This implies that the seismic

245   performance of the dual retrofitted structure (i.e. Phase 4) improved compared to the structure with only PTMS

246   retrofitting. It should be mentioned that, in addition to the CFRP/PTMS-retrofitting, the welding of the

247   longitudinal beam and column bars may have also contributed to enhance the seismic performance of the

248   retrofitted building. However, the similar strain gauge readings recorded during Phase 3 (before welding) and

249   Phase 4 (after welding) at the same PGA=0.30g (Fig. 15) indicate that the welding contribution was negligible

250   when the beam bars were tensioned. Nonetheless, the repairs and the welding have contributed to reducing

27

251 strain in compression after 27 s of shaking when joint damage occurred in Phase 3, as indicated by a sharp

252 increase in compressive strain at that time.
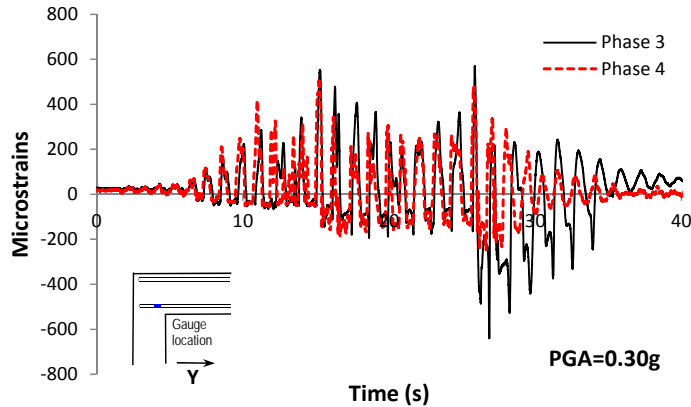
254 **Fig. 15** Comparison of strain gauge readings recorded during Phase 3 (before welding) and Phase 4 (after welding) at
255 PGA=0.30g (frame A)

256 Compared to Phase 4, the *DI* in the Y direction during Phase 5 increased slightly to 0.82 after the first 3D

257 seismic test at PGA=0.10g. Fig. 14 shows that damage in the Y direction remained constant (*DI*=0.82) up to a

258 PGA=0.50g, thus indicating most of the damage in this direction was produced during Phase 4. The *DI* in the

259 X direction was 0.76 at the start of Phase 5, which is only 9% higher than that observed at the end of Phase 1

260 (*DI*=0.70), where the tests were halted due to considerable local damage in the joints. Damage in the X direction

261 increased progressively with the level of PGA up to *DI*=0.85 at PGA=0.60g. Despite the considerable damage

262 accumulated at the end of the 3D tests, none of the frames strengthened with either CFRP sheets or PTMS were

263 near collapse.

264 The global damage index results indicate that damage was well controlled in the PTMS/CFRP-retrofitted

265 building even at high levels of PGA 3D shaking. This confirms that both retrofitting techniques were very

266 effective at maintaining structural stability, thus preventing the potential collapse of the building.

267 ### 3.4 *Performance levels*

268 Current guidelines for seismic assessment and retrofit of existing buildings such as ASCE/SEI 41-06 (ASCE

269 2007) establish limits on acceptable values of maximum interstorey drift ratios, implying that exceeding these

28

270   limits is a violation of a performance objective. According to ASCE/SEI 41-06, maximum transient drift ratios

271   of δ=1.0%, 2.0% and 4.0% correspond to Immediate Occupancy (IO), Life Safety (LS), and Collapse

272   Prevention (CP) performance levels, respectively.

273   Fig. 16a compares the maximum interstorey drift ratios of the 1st and 2nd floor of the CFRP and PTMS-

274   retrofitted frames. The figure includes the results from the two equidistant displacement transducers fixed on

275   each exterior face of the slabs, labelled as "CFRP" and "PTMS" according to the retrofitting technique used on

276   each frame. It is shown that the 1st and 2nd floors of the retrofitted building had similar δs at all PGA levels.

277   This implies that the both CFRP/PTMS retrofitting solutions led to a more uniform damage distribution over

278   the building height, which allowed a better exploitation of the available members' capacity (Hajirasouliha et

279   al. 2012). The building remained safely within the CP performance level during the last test at PGA=0.35g

280   (δ=2.92%). Overall, maximum drift values of the "PTMS" frame were only 2-6% larger than those of the

281   "CFRP" frame, thus indicating that some negligible in-plan torsion occurred during the 3D tests.

282

283

284
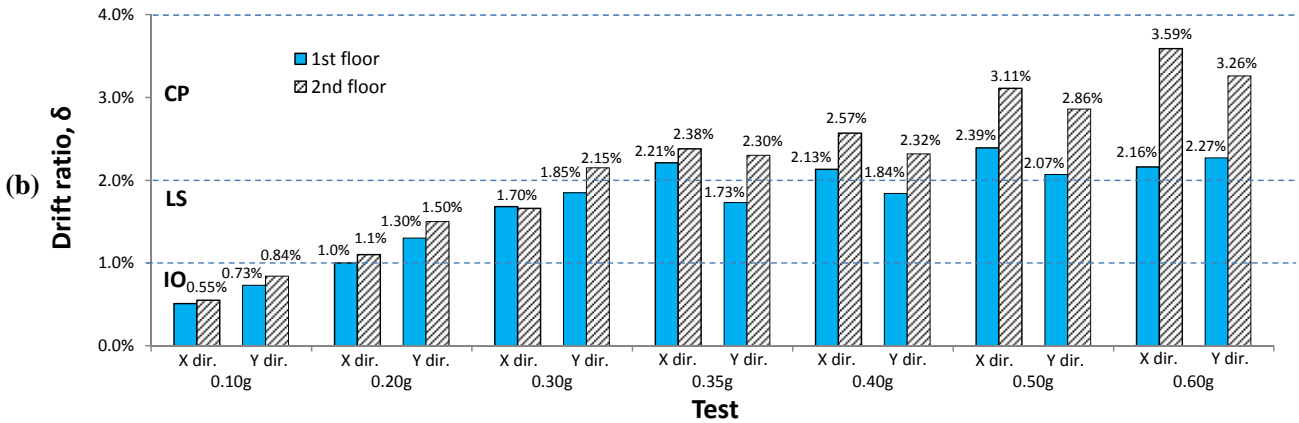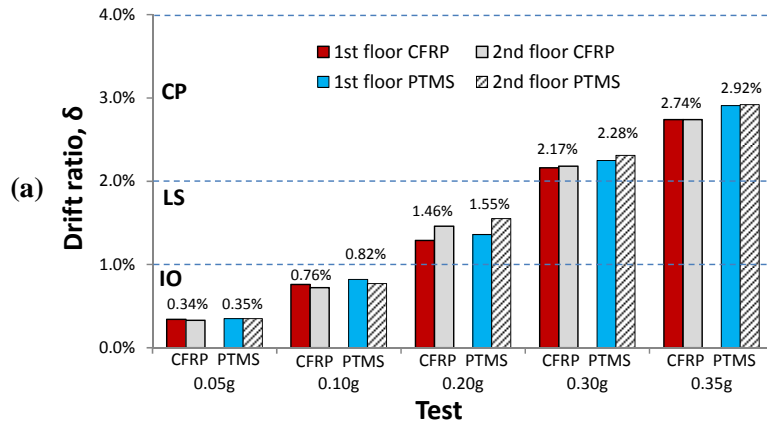
285   **Fig. 16** Interstorey drift ratio of 1st and 2nd floors during (a) Phase 4 (Y dir.), and (b) Phase 5 (3D)

286   Fig. 16b compares maximum interstorey drift ratios for the X and Y directions of the PTMS-retrofitted frame

287   (i.e. the most critical) during Phase 5. At PGA levels between 0.10 and 0.30g, drifts in the Y direction were 10-

288   40% larger than those in the X direction. Conversely, slightly larger drifts were observed in the X direction

289   after a PGA=0.35g. Whilst the drift values measured at the 2nd floor (δ=3.59%) were close to the theoretical

290   CP limit (δ=4.0%) at a PGA=0.60g, the building did not show evidence of structural failure. In comparison to

291   the original bare building (Phase 1), the CFRP/PTMS retrofitting intervention enhanced the maximum drift

292   capacity from 0.82% to 2.16% for the 1st floor (+160%), and from 1.69% to 3.59% for the 2nd floor (+110%).

293   This enhancement in lateral deformation improved considerably the behaviour of the 2nd floor, which was near

294   collapse at a much lower PGA=0.15g during Phase 1.

295 Whilst the building was tested up to a drift level close to the theoretical collapse, the experimental observations

296 indicated that its residual capacity was not yet exhausted. Nonetheless, as it was mentioned before, the tests

297 had to be halted after the test at PGA=0.60g because the maximum displacement limits of the shake table were

298 reached.

3.5 Local strains

300 To assess the effective force taken by the retrofitting solutions, local strains were monitored using foil-type

301 strain gauges fixed on the CFRP sheets and metal straps. Fig. 17 shows the location of two equivalent strain

302 gauges (placed on opposite frames A and B) and their corresponding development of strains during the last test

303 at PGA=0.60g (Phase 5). These are typical results and the following observations apply to all gauges. As shown

304 in Fig. 17, elastic strains of up to 5000 and 1300 $\mu\varepsilon$ were recorded in the CFRP sheets and metal straps,

305 respectively. In all cases, maximum CFRP strains remained below the rupture strain of the sheets, whereas no

306 yielding occurred in the metal straps. Readings from strain gauges fixed on the longitudinal beam bars of the

307 1st floor joints showed that the onset of yielding occurred during Phase 4 at a PGA=0.30g (see Fig. 18), thus

308 confirming that a strong column-weak beam behaviour was achieved in line with current seismic design

309 philosophy. However, yielding was limited as the CFRP/PTMS retrofitting also sustained the tensile forces

310 acting on the beams and columns, as evidenced by the local debonding of the CFRP sheets and shearing off of

311 some metal clips.
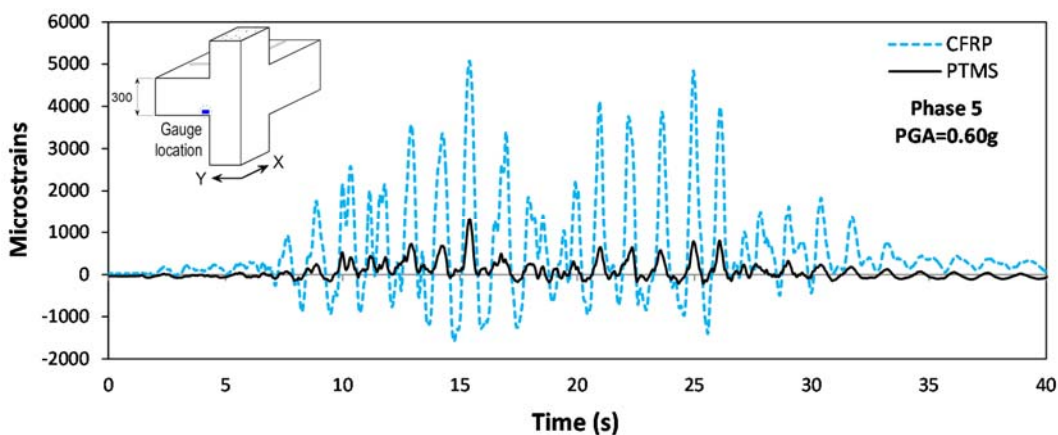
312

313 **Fig. 17** Strain time-history of CFRP sheets and metal straps during 3D test at PGA=0.60g
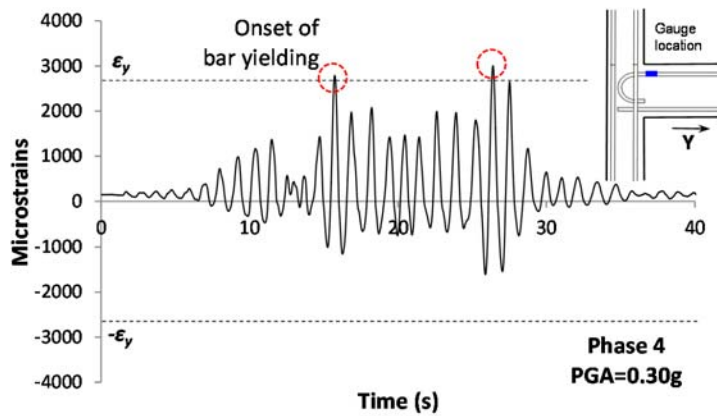
Fig. 18 Strains time-history of longitudinal beam reinforcement in test at PGA=0.30g (Phase 4)

Fig. 19 compares accumulated residual strains from four critical gauges fixed on beams and columns of the CFRP and PTMS frames of the retrofitted building (Phases 4 and 5). For instance, CFRP-B and CFRP-C correspond to gauges located at the beam and column of frame A, respectively. It is shown that, as a result of accumulated damage in the building, the strains in the CFRP sheets increased progressively with the applied PGA up to 1300 µε (PGA=0.60g in Phase 5). Conversely, the residual PTMS strains reduced gradually (up to 400-500 µε at the end of Phase 5) due to some local damage of the push type seals, which led to stress relaxation in the straps. Despite this loss of some tensioning force, it is estimated that the straps maintained 70-80% of their initial force, thus confirming the reliability of the PTMS technique at high seismic excitation levels. Similar levels of tensioning force loss were also observed in tests on lap-spliced beams retrofitted with PTMS (Helal et al. 2014).
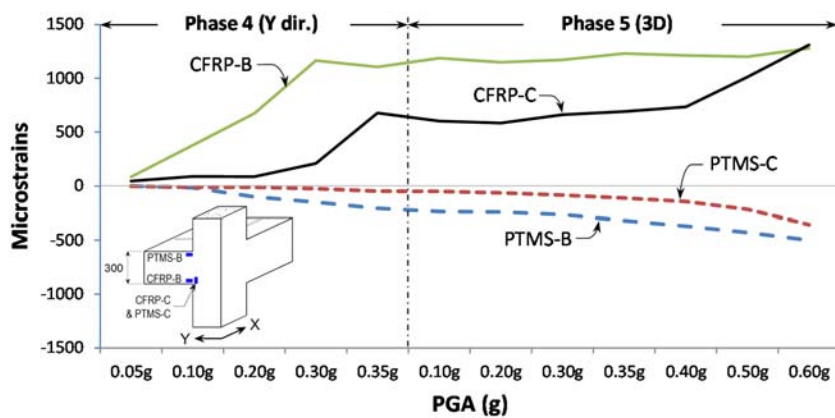
Fig. 19 Accumulated residual strains in CFRP sheets and metal straps

328   Based on the results of Phases 4 and 5, it can be concluded that the dual CFRP/PTMS retrofitting is very

329   effective at enhancing the capacity of substandard RC buildings likely to experience large interstorey drift ratio

330   demands (i.e. close to a CP performance level). Due to the low material costs and ease of installation, the PTMS

331   technique is especially suitable for retrofitting structures, particularly in developing countries. However, the

332   minor damage observed in some of the push type metal seals and bolts at high levels of PGA indicates that

333   further research is necessary to develop more efficient anchorage systems.

4   Conclusions

335   This article examined the effectiveness of CFRP and PTMS retrofitting solutions through full-scale shaking

336   table tests on a substandard RC building. Based on the experimental results, the following conclusions are

337   drawn:

338   1) The initial tests on the original substandard building were halted at a PGA=0.15g to avoid a possible collapse

339   caused by the premature local failure of the beam-column joints at the 2nd floor.

340   2) After significant damage, the local repairs (i.e. crack injection and concrete patching) and dual CFRP/PTMS

341   retrofitting of columns and joints were effective at restoring the lateral stiffness of the building by 75%.

342   3) Whilst the 2nd floor of the original bare structure reached a critical level of damage at PGA=0.15g, the

343   CFRP/PTMS-retrofitted building sustained 3D seismic shaking up to a much higher PGA=0.60g without

344   compromising its stability. The proposed CFRP/PTMS retrofitting intervention also led to a more uniform

345   damage distribution and, therefore, to a better exploitation of the available capacity in the structure.

346   4) In comparison to the original bare building, the retrofitting intervention enhanced the interstorey drift ratio

347   capacity of the 1st and 2nd floors by 160% and 110%, respectively. The building remained safely within the

348   Collapse Prevention performance level and without evidence of potential collapse.

349   5) Although some push type seals sheared off during the tests at high PGA levels (Phase 5), the metal straps

350   maintained 70-80% of their initial post-tensioning force, thus confirming the reliability of the PTMS technique

351 at high seismic excitation levels. Comparatively, the CFRP sheets sustained only local minor debonding. The

352 adopted retrofitting solution also led to a strong column-weak beam behaviour and yielding of the beams at the

353 1st floor, which is in line with current seismic design philosophy.

354 It can be concluded that both CFRP and PTMS retrofitting systems are extremely effective at enhancing the

355 performance of substandard RC structures, and are suitable for retrofitting existing buildings exposed to high

356 seismic hazard. While this article mainly focused on the effectiveness of external reinforcement on exterior

357 joints and columns, the application of the proposed CFRP and PTMS retrofitting systems may be challenging

358 for interior joints. To address this issue, several FRP retrofitting and anchoring solutions are commercially

359 available for interior/exterior columns and joints. The proposed detailing for PTMS strengthening of exterior

360 joints can be also adopted for interior joints; however, more efficient PTMS anchoring solutions could be

361 developed in future research. Further research should also investigate the effectiveness of the anchoring system

362 for the flexural straps on low-strength concrete, where the anchoring bolts may cause damage to the surrounding

363 concrete.

References

367 AFNOR (2007) Aciers pour beton arrne - Aciers soudables a verrous Partie1: Barres et couronnes. NF A 35-016-1,.
368   Association Française de Normalisation, Paris
369 Akguzel U, Pampanin S (2010) Effects of variation of axial load and bidirectional loading on seismic performance of
370   GFRP retrofitted reinforced concrete exterior beam-column joints. J Compos Constr 14 (1):94-104.
371   doi:10.1061/(Asce)1090-0268(2010)14:1(94)
372 Al-Salloum YA, Almusallam TH, Alsayed SH, Siddiqui NA (2011) Seismic behavior of as-built, ACI-complying, and
373   CFRP-repaired exterior RC beam-column joints. J Compos Constr 15 (4):522-534. doi:10.1061/(Asce)Cc.1943-
374   5614.0000186
375 Antonopoulos CP, Triantafillou TC (2003) Experimental investigation of FRP-strengthened RC beam-column joints. J
376   Compos Constr 7 (1):39-49. doi:10.1061/(Asce)1090-0268(2003)7:1(39)
377 ASCE (2007) ASCE/SEI 41-06 Seismic rehabilitation of existing buildings. American Society of Civil Engineers, Reston,
378   VA
379 Biddah A, Ghobarah A, Aziz TS (1997) Upgrading of nonductile reinforced concrete frame connections. J Struct Eng 123
380   (8):1001-1010
381 CEN (2004a) EN 1992-1-1:2004. Eurocode 2: Design of concrete structures, Part 1-1: General rules and rules for
382   buildings. Comité Européen de Normalisation, Lausanne
383 CEN (2004b) EN 1998-1:2004 Eurocode 8 - Design of structures for earthquake resistance Part 1: General rules, seismic
384   actions and rules for buildings. Comité Européen de Normalisation, Lausanne
385 CEN (2009a) EN 12390-5:2009 Testing hardened concrete Part 5: Flexural strength of test specimens. Comité Européen
386   de Normalisation. Lausanne, Switzerland

387   CEN (2009b) EN 12390-6:2009 Testing hardened concrete Part 6: Tensile splitting strength of test specimens. Comité
388   Européen de Normalisation,. Lausanne, Switzerland
389   Clough RW, Penzien J (2003) Dynamics of structures. Computers & Structures, Inc, Berkeley, CA
390   Corazao M, Durrani AJ (1989) Repair and strengthening of beam-to-column connections subjected to earthquake loading.
391   National Center for Earthquake Engineering Research, State University of New York at Buffalo,
392   DiPasquale E, Ju JW, Askar A, Cakmak AS (1990) Relation between global damage indexes and local Stiffness
393   degradation. J Struct Eng-Asce 116 (5):1440-1456. doi:10.1061/(Asce)0733-9445(1990)116:5(1440)
394   Frangou M (1996) Strengthening of concrete by lateral confinement. Ph.D. thesis, Dept. of Civil and Structural
395   Engineering, The University of Sheffield, UK
396   Frangou M, Pilakoutas K, Dritsos S (1995) Structural repair strengthening of RC columns. Cons Build Mater 9 (5):259-
397   266. doi:10.1016/0950-0618(95)00013-6
398   Garcia R, Hajirasouliha I, Guadagnini M, Helal Y, Jemaa Y, Pilakoutas K, Mongabure P, Chrysostomou C, Kyriakides
399   N, Ilki A, Budescu M, Taranu N, Ciupala MA, Torres L, Saiidi M (2014a) Full-scale shaking table tests on a
400   substandard RC building repaired and strengthened with Post-Tensioned Metal Straps. Journal of Earthquake
401   Engineering 18 (2):187-213. doi:10.1080/13632469.2013.847874
402   Garcia R, Hajirasouliha I, Pilakoutas K (2010) Seismic behaviour of deficient RC frames strengthened with CFRP
403   composites. Eng Struct 32 (10):3075-3085. doi:10.1016/j.engstruct.2010.05.026
404   Garcia R, Helal Y, Pilakoutas K, Guadagnini M (2014b) Bond behaviour of substandard splices in RC beams externally
405   confined with CFRP. Construction and Building Materials 50:340-351
406   Garcia R, Helal Y, Pilakoutas K, Guadagnini M (2015) Bond strength of short lap splices in RC beams confined with steel
407   stirrups or external CFRP. Materials and Structures 48 (1-2):277-293. doi:10.1617/s11527-013-0183-5
408   Garcia R, Jemaa Y, Helal Y, Guadagnini M, Pilakoutas K (2014c) Seismic strengthening of severely damaged beam-
409   column RC joints using CFRP. J Compos Constr 18 (2). doi:10.1061/(Asce)Cc.1943-5614.0000448
410   Gdoutos EE, Pilakoutas K, Rodopoulos CA (2000) Failure analysis of industrial composite materials. McGraw-Hill New
411   York,
412   Ghobarah A, Aziz TS, Biddah A (1996) Seismic rehabilitation of reinforced concrete beam-column connections.
413   Earthquake Spectra 12 (4):761-780. doi:10.1193/1.1585909
414   Ghobarah A, El-Amoury T (2005) Seismic rehabilitation of deficient exterior concrete frame joints. J Compos Constr 9
415   (5):408-416. doi:10.1061/(Asce)1090-0268(2005)9:5(408)
416   Hajirasouliha I, Asadi P, Pilakoutas K (2012) An efficient performance-based seismic design method for reinforced
417   concrete frames. Earthq Eng Struct D 41 (4):663-679. doi:10.1002/Eqe.1150
418   Helal Y (2012) Seismic strengthening of deficient RC elements using PTMS. Ph.D. thesis, Dept. of Civil and Structural
419   Engineering, The University of Sheffield, UK
420   Helal Y, Garcia R, Guadagnini M, Pilakoutas K, Hajirasouliha I (2014) Strengthening of short splices in RC beams using
421   post-tensioned metal straps. Materials and Structures - (-):1-15. doi:10.1617/s11527-014-0481-6
422   Ilki A, Bedirhanoglu I, Kumbasar N (2011) Behavior of FRP-retrofitted joints built with plain bars and low-strength
423   concrete. J Compos Constr 15 (3):312-326. doi:10.1061/(ASCE)CC.1943-5614.0000156
424   Karayannis CG, Chalioris CE, Sirkelis GM (2008) Local retrofit of exterior RC beam-column joints using thin RC jackets
425   - An experimental study. Earthq Eng Struct Dyn 37 (5):727-746. doi:10.1002/Eqe.783
426   Kyriakides N, Ahmad S, Pilakoutas K, Neocleous K, Chrysostomou C (2014) A probabilistic analytical seismic
427   vulnerability assessment framework for substandard structures in developing countries. Earthq Struct 6 (6):665-
428   687
429   Li JB, Gong JX, Wang LC (2009) Seismic behavior of corrosion-damaged reinforced concrete columns strengthened using
430   combined carbon fiber-reinforced polymer and steel jacket. Cons Build Mater 23 (7):2653-2663.
431   doi:10.1016/j.conbuildmat.2009.01.003
432   Ministry of Construction of China (2001) Code for seismic design of buildings (GB50011-2001). China Architecture and
433   Building Press, Beijing
434   Moghaddam H, Samadi M, Pilakoutas K, Mohebbi S (2010) Axial compressive behavior of concrete actively confined by
435   metal strips; part A: experimental study. Mater Struct 43 (10):1369-1381. doi:10.1617/s11527-010-9588-6
436   Mongabure P (2012) BANDIT project: seismic tests on a reinforced concrete frame with post-tensioned metal strips
437   retrofitting, final report. FP7 SERIES Programme (Seismic Engineering Research Infrastructures for European
438   Synergies).
439   Pantelides CP, Gergely J (2008) Seismic retrofit of reinforced concrete beam column T-joints in bridge piers with FRP
440   composite jackets. Paper presented at the SP-258: Seismic Strengthening of Concrete Buildings Using FRP
441   Composites (in CD-ROM),
442   Parvin A, Altay S, Yalcin C, Kaya O (2010) CFRP rehabilitation of concrete frame joints with inadequate shear and
443   anchorage details. J Compos Constr 14 (1):72-82. doi:10.1061/(Asce)Cc.1943-5614.0000055

444 RILEM (1994) RILEM Recommendations for the testing and use of constructions materials - CPC 8 modulus of elasticity
445   of concrete in compression 1975.
446 Sasmal S, Ramanjaneyulu K, Novak B, Srinivas V, Kumar KS, Korkowski C, Roehm C, Lakshmanan N, Iyer NR (2011)
447   Seismic retrofitting of nonductile beam-column sub-assemblage using FRP wrapping and steel plate jacketing.
448   Cons Build Mater 25 (1):175-182. doi:10.1016/j.conbuildmat.2010.06.041
449 Sezen H (2012) Repair and strengthening of reinforced concrete beam-column joints with Fiber-Reinforced Polymer
450   Composites. J Compos Constr 16 (5):499-506. doi:10.1061/(Asce)Cc.1943-5614.0000290
451 Thermou GE, Pantazopoulou SJ (2011) Assessment indices for the seismic vulnerability of existing RC buildings. Earthq
452   Eng Struct D 40 (3):293-313. doi:10.1002/Eqe.1028
453 Tsonos ADG (2010) Performance enhancement of R/C building columns and beam-column joints through shotcrete
454   jacketing. Eng Struct 32 (3):726-740. doi:10.1016/j.engstruct.2009.12.001
455 Zembaty Z, Kowalski M, Pospisil S (2006) Dynamic identification of a reinforced concrete frame in progressive states of
456   damage. Eng Struct 28 (5):668-681. doi:10.1016/j.engstruct.2005.09.025

457

458